
One Positive Label is Sufficient: Single-Positive Multi-Label Learning with Label Enhancement

Ning Xu¹, Congyu Qiao¹, Jiaqi Lv², Xin Geng^{1*}, Min-Ling Zhang¹

¹School of Computer Science and Engineering, Southeast University, Nanjing 210096, China

²RIKEN Center for Advanced Intelligence Project, Tokyo 103-0027, Japan

{xning, qiaocy}@seu.edu.cn, is.jiaqi.lv@gmail.com,

{xgeng, zhangml}@seu.edu.cn

Abstract

Multi-label learning (MLL) learns from the examples each associated with multiple labels simultaneously, where the high cost of annotating all relevant labels for each training example is challenging for real-world applications. To cope with the challenge, we investigate single-positive multi-label learning (SPMLL) where each example is annotated with only one relevant label and show that one can successfully learn a theoretically grounded multi-label classifier on SPMLL training examples. In this paper, a novel SPMLL method named SMILE, i.e., Single-positive Multi-label learning with Label Enhancement, is proposed. Specifically, an unbiased risk estimator is derived, which could be guaranteed to approximately converge to the optimal risk minimizer in fully supervised learning and shows that one positive label of each instance is sufficient to train a model. Then, the corresponding empirical risk estimator is established via recovering the latent soft label as a label enhancement process, where the posterior density of the latent soft labels is approximate to the variational Beta density parameterized by an inference model. Experiments on twelve corrupted MLL datasets show the effectiveness of SMILE over several existing SPMLL approaches. Source code is available at <https://github.com/palm-ml/smile>.

1 Introduction

Multi-label learning (MLL) aims to build a predictive model to assign a set of relevant labels for the unseen instance via learning from the training examples associated with multiple class labels simultaneously [30, 46]. During the past decade, MLL has been widely applied to learn from the data containing rich semantics, such as multimedia content annotation [40, 33], text categorization [29, 27], music emotion analysis [21, 35], and bioinformatics analysis [3], etc.

However, in practice, obtaining ground-truth multiple labels for MLL training datasets is costly due to the expensive and time-consuming manual annotations. Comparing with multi-class learning where an example is associated with only *one positive label*, multi-label learning requires the *complete positive label set* for each example. On this account, the annotation cost of multi-label learning is significantly higher than multi-class classification, which limits its application especially when the number of categories is large.

To mitigate this problem, the setting of single-positive multi-label learning (SPMLL) [5] allows for significantly reduced annotations costs for the datasets, where each example is annotated with

*Corresponding author

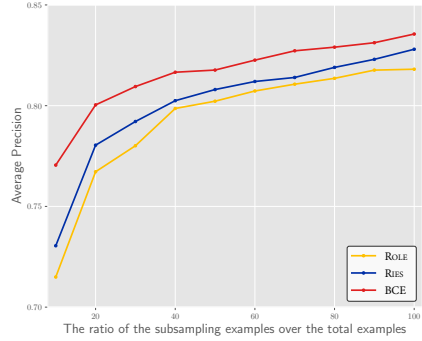


Figure 1: Test average precision on tmc2007. Each curve is generated by randomly subsampling the examples from the training set, where BCE is trained on fully labeled examples via binary cross-entropy loss while the SPMLL methods (ROLE [5] and the proposed SMILE) are trained on single-positive case.

only one relevant label. In Figure 1, comparing with fully labeled case, the SPMLL approaches on single-positive labeled examples only incur a tolerable drop in the performance but drastically reduce the amount of supervision required to train multi-label classifiers. By establishing the SPMLL methods with the learning power of DNNs, recent work [5] has also empirically validated that SPMLL would reduce the annotations costs while achieving good performance in practice. However, no method could provide theoretical insights as to why the model trained on the SPMLL examples can converge to an ideal one.

In this paper, we propose a theoretically-guaranteed method named SMILE, i.e., Single-positive Multi-label learning with Label Enhancement. Specifically, we first derive an unbiased risk estimator, which suggests that one positive label of each instance is sufficient to train the predictive models for multi-label learning. Besides, an estimation error bound is derived, which guarantees the risk-consistency [25] of the proposed method. Then we could design a benchmark solution via recovering the soft labels corresponding to each example in a label enhancement process [39, 36], where the posterior density of the latent soft labels is inferred by leveraging an approximate Beta density. The contributions are summarized as follows:

- Theoretically, we for the first time derive an unbiased risk estimator for SPMLL. Based on this, an estimation error bound is established that guarantees the risk-consistency and demonstrates that the obtained risk minimizer in SPMLL would approximately converge to the optimal risk minimizer in fully supervised MLL.
- Practically, we propose the method SMILE for SPMLL via adopting the latent soft labels recovered by label enhancement. The posterior density of the latent soft label is inferred by leveraging an approximate Beta density and the evidence lower bound (ELBO) [18] for the optimization is deduced.

Experiments on twelve corrupted MLL datasets show the effectiveness of SMILE over several existing SPMLL approaches.

2 Related Work

In multi-label learning, each example is associated with multiple class labels simultaneously. As the output space in MLL is exponential in size to the number of class labels, numerous approaches are proposed to exploit the label correlations to promote the learning process [14, 44, 31]. The first-order approaches disassemble the MLL problem into a number of binary classification problems [2, 45]. The second-order approaches consider the label correlations between pairs of labels [8, 11]. The high-order approaches further focus on the label correlations among the label set [26, 32]. Another line of research focuses on manipulating the feature space via formalizing label-specific feature to each class label to facilitate multi-label classification [23, 15, 42]. In addition, some work focus on dealing with MLL via deep models. A directed graph over the labels is established via employing

GCN to propagate information among all label nodes [4]. Transformer is leveraged for exploring the label dependency by introducing a ternary encoding scheme to represent the state of labels [20].

In practice, the labeling information is often incomplete in training data, since acquiring exhaustive supervision is extremely difficult. Numerous approaches have been proposed to handle the MLL with missing labels [12], which is also termed as MLL with partial labels [7]. A transductive learning method is proposed to concatenate features and labels and apply the matrix completion technique to it [12]. Then, the inductive learning method is proposed to exploit the structure of specific loss functions to offer efficient algorithms for learning with missing labels [41]. Wu [34] recovers the full labeling information of each training sample via enforcing consistency with available label-assignment and smoothness of label-assignment. The global and local label correlations are exploited simultaneously via learning a latent label representation in the missing label cases [47]. Durand [7] empirically compare different label-assignment strategies to show the potential to employ partial labels for MLL. Another method induces a cost function that measures the smoothness of labels and features to alleviate the overfitting issue when training data contains missing labels [16].

Comparing with multi-label learning with missing labels, SPMLL [5] considers the hardest version of this problem, where annotators are only asked to provide a single positive label for each training example and no additional negative or positive labels. When collecting multi-label annotations, it may be more efficient to annotate only one label rather than multiple labels for each example. To learn from SPMLL examples, an intuitive solution is “assume negative” (AN) [5], which assumes that unobserved labels are negative and trains the predictive model with binary cross-entropy loss on observed positive labels. Recent work [5] proposes some methods to reduce the damaging effects of false-negative labels. An expected positive regularization [5] is proposed to avoid the problem but the expected number of positive labels of each example should be given. Label smoothing [28] is employed to reduce the impact of the incorrect labels. Another approach [5] estimates the unobserved labels and encourages the classifier predictions to match the estimated labels via binary entropy loss. However, no methods can provide theoretical insights as to why the model trained on SPMLL examples can converge to an ideal one.

3 Problem Setup

3.1 Multi-Label Learning

In MLL, each example is associated with multiple labels, and aims to build a predictive model which can assign a set of relevant labels for the unseen instance. Let $\mathcal{X} = \mathbb{R}^q$ be the q -dimensional instance space and $\mathcal{Y} = \{1, 2, \dots, c\}$ be the label space with c class labels. Given the MLL training set $\mathcal{D} = \{(\mathbf{x}_i, Y_i) | 1 \leq i \leq n\}$ where $\mathbf{x}_i \in \mathcal{X}$ denotes the q -dimensional instance and $Y_i \in \mathcal{C}$ is the set of relevant labels associated with \mathbf{x}_i where $\mathcal{C} = 2^{\mathcal{Y}}$. The task of multi-label learning is to induce a multi-label classifier $f : \mathcal{X} \mapsto 2^{\mathcal{Y}}$ that minimizes the following classification risk:

$$R(f) = \mathbb{E}_{p(\mathbf{x}, Y)} [\mathcal{L}(f(\mathbf{x}), Y)]. \quad (1)$$

Here, $\mathcal{L} : \mathbb{R}^q \times 2^{\mathcal{Y}} \mapsto \mathbb{R}_+$ is a multi-label loss function that measures how well the model fits the data. Note that a method is risk-consistent if the method possesses a classification risk estimator that is equivalent to $R(f)$ given the same classifier f [25, 9].

3.2 Single-Positive Multi-Label Learning

Given the SPMLL training set $\tilde{\mathcal{D}} = \{(\mathbf{x}_i, \gamma_i) | 1 \leq i \leq n\}$ where $\gamma_i \in \mathcal{Y}$ denotes the observed single-positive label of \mathbf{x}_i . Note that $\gamma_i \in Y_i$ while its relevant label set Y_i is not directly accessible to the learning algorithms. For each SPMLL training example (\mathbf{x}_i, γ_i) , we use the observed single-positive vector $\mathbf{l}_i = [l_i^1, l_i^2, \dots, l_i^c]^\top \in \{0, 1\}^c$ to represent whether j -th label is the observed positive label, i.e., $l_i^j = 1$ if $j = \gamma_i$, otherwise $l_i^j = 0$. The multi-label vector is denoted by $\mathbf{y}_i = [y_i^1, y_i^2, \dots, y_i^c]^\top \in \{0, 1\}^c$, where $y_i^j = 1$ if the j -th label is relevant to \mathbf{x}_i and $y_i^j = 0$ if the j -th label is irrelevant. The task of SPMLL is to induce a multi-label classifier $f : \mathcal{X} \mapsto 2^{\mathcal{Y}}$ from $\tilde{\mathcal{D}}$, which can assign a set of relevant label set for the unseen instance.

Recent work [5] empirically validates that SPMLL would reduce the amount of supervision with a tolerable damage in classification performance. The intuitive solution AN is assuming that unobserved

labels are negative, which leads to the drawback that introduces some number of false negative labels. Therefore, the SOTA approaches [5] aim to reduce the damaging effects of false-negative labels via employing the learning power of DNNs to achieve good performance in practice. However, there is no existing method that can provide theoretical insights.

4 The Proposed Method

4.1 Risk-Consistent Estimator

To deal with single-positive multi-label learning, the classification risk $R(f)$ in Eq. (1) could be rewritten as

$$\begin{aligned}
& \mathbb{E}_{p(\mathbf{x}, Y)} [\mathcal{L}(f(\mathbf{x}), Y)] \\
&= \int_{\mathbf{x}} \sum_{Y \in \mathcal{C}} \mathcal{L}(f(\mathbf{x}), Y) p(Y|\mathbf{x}) p(\mathbf{x}) d\mathbf{x} \\
&= \int_{\mathbf{x}} \sum_{\gamma \in \mathcal{Y}} \sum_{Y \in \mathcal{C}} \mathcal{L}(f(\mathbf{x}), Y) \frac{p(Y|\mathbf{x})}{p(y^\gamma = 1|\mathbf{x})^c} p(y^\gamma = 1|\mathbf{x}) p(\mathbf{x}) d\mathbf{x} \\
&= \mathbb{E}_{p(\mathbf{x}, \gamma)} \left[\frac{1}{p(y^\gamma = 1|\mathbf{x})^c} \sum_{Y \in \mathcal{C}} \mathcal{L}(f(\mathbf{x}), Y) p(Y|\mathbf{x}) \right] \\
&= R_{sp}(f).
\end{aligned} \tag{2}$$

Additionally, we employ the widely used loss function in multi-label learning, i.e, binary cross-entropy loss, as the loss function $\mathcal{L}(f(\mathbf{x}), Y)$:

$$\begin{aligned}
\mathcal{L}(f(\mathbf{x}), Y) &= \sum_{j \in Y} \log f_j(\mathbf{x}) + \sum_{j \notin Y} \log(1 - f_j(\mathbf{x})) \\
&= \sum_{j \in Y} \ell^j + \sum_{j \notin Y} \bar{\ell}^j,
\end{aligned} \tag{3}$$

where $\ell^j = \log f_j(\mathbf{x})$ and $\bar{\ell}^j = \log(1 - f_j(\mathbf{x}))$. Then, $\sum_{Y \in \mathcal{C}} \mathcal{L}(f(\mathbf{x}), Y) p(Y|\mathbf{x})$ in Eq. (2) could be calculated as¹

$$\sum_{Y \in \mathcal{C}} \mathcal{L}(f(\mathbf{x}), Y) p(Y|\mathbf{x}) = \sum_{j=1}^c d^j \ell^j + (1 - d^j) \bar{\ell}^j. \tag{4}$$

Here, $d^j = p(y^j = 1|\mathbf{x}) \in [0, 1]$ would be regarded as the soft label corresponding to class j for \mathbf{x} . By substituting Eq. (4) into Eq. (2), we obtain the following risk-consistent estimator for SPMLL

$$R_{sp}(f) = \mathbb{E}_{p(\mathbf{x}, \gamma)} \left[\frac{1}{p(y^\gamma = 1|\mathbf{x})^c} \sum_{j=1}^c d^j \ell^j + (1 - d^j) \bar{\ell}^j \right]. \tag{5}$$

Therefore, we could express the empirical risk estimator via

$$\hat{R}_{sp}(f) = \frac{1}{n} \sum_{i=1}^n \left(\frac{1}{p(y^{\gamma^i} = 1|\mathbf{x}_i)^c} \sum_{j=1}^c d_i^j \ell_i^j + (1 - d_i^j) \bar{\ell}_i^j \right). \tag{6}$$

Then, we could design a benchmark solution via applying the sigmoid function on $f_{\gamma_i}(\mathbf{x}_i)$ to approximate $p(y^{\gamma_i} = 1|\mathbf{x}_i)$ and recovering the soft label d_i^j corresponding to each example via the label enhancement process in the following subsection.

4.2 Training with Label Enhancement

To recover the soft label vector $\mathbf{d}_i = [d_i^1, d_i^2, \dots, d_i^c]^\top \in [0, 1]^c$, SMILE considers the topological information of the feature space and estimates adjacency matrix $\mathbf{A} = [a_{ij}]_{n \times n}$ with

$$a_{ij} = \begin{cases} 1 & \text{if } \mathbf{x}_i \in \mathcal{N}(\mathbf{x}_j) \\ 0 & \text{otherwise} \end{cases}, \tag{7}$$

¹The detail is provided in Appendix A.

where $\mathcal{N}(\mathbf{x}_j)$ is the set for k -nearest neighbors of \mathbf{x}_j .

We assume that the latent soft label matrix $\mathbf{D} = [\mathbf{d}_1, \mathbf{d}_2, \dots, \mathbf{d}_n]$ generates the observed logical label matrix $\mathbf{L} = [l_1, l_2, \dots, l_n]$ and the adjacency matrix \mathbf{A} . Besides, the observed instance matrix $\mathbf{X} = [\mathbf{x}_1, \mathbf{x}_2, \dots, \mathbf{x}_n]$ is generated from \mathbf{D} and the latent feature matrix $\mathbf{Z} = [\mathbf{z}_1, \mathbf{z}_2, \dots, \mathbf{z}_n]$. We assume that the prior density $p(\mathbf{d})$ is a Beta density with the minor values $\hat{\alpha} = [\hat{\alpha}^1, \hat{\alpha}^2, \dots, \hat{\alpha}^c]$ and $\hat{\beta} = [\hat{\beta}^1, \hat{\beta}^2, \dots, \hat{\beta}^c]$, i.e., $p(\mathbf{d}) = \prod_{j=1}^c \text{Beta}(d^j | \hat{\alpha}^j, \hat{\beta}^j)$. Then the prior density $p(\mathbf{D})$ could be the product of each $p(\mathbf{d})$. In addition, We assume that the prior density $p(\mathbf{z})$ is a standard Gaussian and prior density $p(\mathbf{Z})$ can be represented as the product of each Gaussian $p(\mathbf{Z}) = \prod_{i=1}^n \text{Gau}(\mathbf{z}_i | \mathbf{0}, \mathbf{1})$. Then, the posterior density $p(\mathbf{D}, \mathbf{Z} | \mathbf{L}, \mathbf{X}, \mathbf{A})$ can be decomposed as follows:

$$p(\mathbf{D}, \mathbf{Z} | \mathbf{L}, \mathbf{X}, \mathbf{A}) = p(\mathbf{D} | \mathbf{L}, \mathbf{X}, \mathbf{A}) p(\mathbf{Z} | \mathbf{D}, \mathbf{L}, \mathbf{X}, \mathbf{A}) = p(\mathbf{D} | \mathbf{L}, \mathbf{X}, \mathbf{A}) p(\mathbf{Z} | \mathbf{D}, \mathbf{X}) \quad (8)$$

where \mathbf{L} and \mathbf{A} can be removed from the condition of $p(\mathbf{Z} | \mathbf{D}, \mathbf{L}, \mathbf{X}, \mathbf{A})$ because of the independence between \mathbf{Z} and \mathbf{L}, \mathbf{A} when latent variable \mathbf{D} is given in the condition. Here we employ $q(\mathbf{D} | \mathbf{L}, \mathbf{X}, \mathbf{A})$ and $q(\mathbf{Z} | \mathbf{D}, \mathbf{X})$ to approximate the true posterior $p(\mathbf{D} | \mathbf{L}, \mathbf{X}, \mathbf{A})$ and $p(\mathbf{Z} | \mathbf{D}, \mathbf{X})$ respectively. The approximate posterior $q(\mathbf{D} | \mathbf{L}, \mathbf{X}, \mathbf{A})$ could be the product of Beta parameterized by $\alpha_i = [\alpha_i^1, \alpha_i^2, \dots, \alpha_i^c]^\top$ and $\beta_i = [\beta_i^1, \beta_i^2, \dots, \beta_i^c]^\top$:

$$q_{w_1}(\mathbf{D} | \mathbf{L}, \mathbf{X}, \mathbf{A}) = \prod_{i=1}^n \prod_{j=1}^c \text{Beta}(d_i^j | \alpha_i^j, \beta_i^j). \quad (9)$$

Here, the parameters $\Delta = [\alpha_1, \alpha_2, \dots, \alpha_n]$ and $\Phi = [\beta_1, \beta_2, \dots, \beta_n]$ are the outputs of the inference model parameterized by w_1 as a GCN [19] with adjacency matrix by \mathbf{A} . Let $q_{w_2}(\mathbf{Z} | \mathbf{D}, \mathbf{X})$ be the product of Gaussian parameterized by the mean vector μ_i and standard deviation vector σ_i :

$$q_{w_2}(\mathbf{Z} | \mathbf{D}, \mathbf{X}) = \prod_{i=1}^n \text{Gau}(\mathbf{z}_i | \mu_i, \sigma_i), \quad (10)$$

The parameters $\Lambda = [\mu_1, \mu_2, \dots, \mu_n, \sigma_1, \sigma_2, \dots, \sigma_n]$ are the outputs of the inference model with a MLP parameterized by w_2 .

We derive the evidence lower bound (ELBO) [18] on the marginal likelihood of the model to ensure that $q_w(\mathbf{D}, \mathbf{Z} | \mathbf{L}, \mathbf{X}, \mathbf{A})$ is as close as possible to $p(\mathbf{D}, \mathbf{Z} | \mathbf{L}, \mathbf{X}, \mathbf{A})$ ¹:

$$\begin{aligned} \mathcal{L}_{ELBO} &= \mathbb{E}_{q_w(\mathbf{D}, \mathbf{Z} | \mathbf{L}, \mathbf{X}, \mathbf{A})} [\log p(\mathbf{X} | \mathbf{D}, \mathbf{Z}) + \log p(\mathbf{L} | \mathbf{D}) + \log p(\mathbf{A} | \mathbf{D})] \\ &\quad - \text{KL}[q_{w_1}(\mathbf{D} | \mathbf{L}, \mathbf{X}, \mathbf{A}) || p(\mathbf{D})] - \text{KL}[q_{w_2}(\mathbf{Z} | \mathbf{D}, \mathbf{X}) || p(\mathbf{Z})]. \end{aligned} \quad (11)$$

We further assume that $p(\mathbf{X} | \mathbf{D}, \mathbf{Z})$ is a product of each Gaussian with means ξ_i and $p(\mathbf{L} | \mathbf{D})$ is a product of each multivariate Bernoulli with probabilities τ_i . In order to simplify the observation model, $\mathbf{T}^{(m)} = [\tau_1^{(m)}, \tau_2^{(m)}, \dots, \tau_n^{(m)}]$ is computed from m -th sampling $\mathbf{D}^{(m)}$ with a MLP parameterized by η_1 and $\Xi^{(m)} = [\xi_1^{(m)}, \xi_2^{(m)}, \dots, \xi_n^{(m)}]$ is computed from m -th sampling $\mathbf{D}^{(m)}$ and $\mathbf{Z}^{(m)}$ with a MLP parameterized by η_2 . Then the first part of Eq. (11) can be tractable as

$$\begin{aligned} \mathbb{E}_{q_w(\mathbf{D}, \mathbf{Z} | \mathbf{L}, \mathbf{X}, \mathbf{A})} [\log p(\mathbf{X} | \mathbf{D}, \mathbf{Z}) + \log p(\mathbf{L} | \mathbf{D}) + \log p(\mathbf{A} | \mathbf{D})] &= \frac{1}{M} \sum_{m=1}^M \text{tr}(\mathbf{L}^\top \log \mathbf{T}^{(m)}) \\ &\quad + \text{tr}((\mathbf{I} - \mathbf{L})^\top \log(\mathbf{I} - \mathbf{T}^{(m)})) - \|\mathbf{A} - S(\mathbf{D}^{(m)} \mathbf{D}^{(m)\top})\|_F^2 + \|\Xi^{(m)} - \mathbf{X}\|_F^2 \end{aligned} \quad (12)$$

Here, $S(\cdot)$ is the logistic sigmoid function, and implicit reparameterization trick [10] and MC sampling [18, 37, 38] are employed.

The second part of Eq. (11) can be analytically calculated as

$$\begin{aligned} \text{KL}(q_{w_1}(\mathbf{D} | \mathbf{L}, \mathbf{X}, \mathbf{A}) || p(\mathbf{D})) &= \sum_{i=1}^n \sum_{j=1}^c \log \frac{\Gamma(\alpha_i^j + \beta_i^j) \Gamma(\hat{\alpha}_i^j) \Gamma(\hat{\beta}_i^j)}{\Gamma(\hat{\alpha}_i^j + \hat{\beta}_i^j) \Gamma(\alpha_i^j) \Gamma(\beta_i^j)} + (\alpha_i^j - \hat{\alpha}_i^j) \psi(\alpha_i^j) \\ &\quad - (\alpha_i^j - \hat{\alpha}_i^j + \beta_i^j - \hat{\beta}_i^j) \psi(\alpha_i^j + \beta_i^j) + (\beta_i^j - \hat{\beta}_i^j) \psi(\beta_i^j). \end{aligned} \quad (13)$$

¹The detail is provided in Appendix B.

Algorithm 1 SMILE Algorithm

Input: The SPMLL training set $\tilde{\mathcal{D}} = \{(\mathbf{x}_i, \gamma_i)\}_{i=1}^n$, the number of iteration I and the number of epoch T ;

- 1: Warm-up θ by using AN solution, and initialize the reference model w_1 , w_2 and observation model η ;
- 2: Estimate the adjacency matrix \mathbf{A} by Eq. (7);
- 3: **for** $t = 1, \dots, T$ **do**
- 4: Shuffle training set $\tilde{\mathcal{D}} = \{(\mathbf{x}_i, \gamma_i)\}_{i=1}^n$ into I mini-batches;
- 5: **for** $k = 1, \dots, I$ **do**
- 6: Update w_1 , w_2 and η by forward computation and back-propagation by Eq. (16);
- 7: Obtain the soft label d_i for each example \mathbf{x}_i by Eq. (9);
- 8: Apply the sigmoid function on $f_{\gamma_i}(\mathbf{x}_i)$ to approximate $p(y^{\gamma_i} = 1|\mathbf{x}_i)$;
- 9: Update θ by forward computation and back-propagation by Eq. (6);
- 10: **end for**
- 11: **end for**

Output: The predictive model θ .

Here, $\Gamma(\cdot)$ and $\psi(\cdot)$ are Gamma function and Digamma function, respectively. The third part of Eq. (11) can be analytically calculated as follows:

$$\text{KL}(q_{w_2}(\mathbf{Z}|\mathbf{D}, \mathbf{X})||p(\mathbf{Z})) = \sum_{i=1}^n \sum_{j=1}^J \left(1 + \log\left((\sigma_i^j)\right) - (\mu_i^j)^2 - (\sigma_i^j)^2 \right). \quad (14)$$

Besides, we could promote the label enhancement process via enforcing that the estimated \mathbf{D} should inherit the labeling-information of observed labels:

$$T_C = -\frac{1}{n} \sum_{i=1}^n \sum_{j=1}^c l_i^j \log d_i^j + \left(1 - l_i^j\right) \left(1 - \log d_i^j\right). \quad (15)$$

Finally, the objective of label enhancement T_{LE} is obtained:

$$T_{LE} = -\lambda \mathcal{L}_{ELBO} + T_C, \quad (16)$$

where λ is a hyper-parameter.

SMILE first initializes the predictive network by warm-up training with AN solution, which would attain a fine network before it starts fitting noise [43]. Then we could sample the soft label from fixed Beta after label enhancement and the sigmoid function on $f_{\gamma_i}(\mathbf{x}_i)$ to approximate $p(y^{\gamma_i} = 1|\mathbf{x}_i)$ to make Eq. (6) accessible, and train the predictive model θ by minimizing the risk estimator. In each epoch, SMILE alternately operates label enhancement process and classifier training process. Algorithm 1 shows the algorithmic description of SMILE.

4.3 Estimation Error Bound

In this subsection, we establish an estimation error bound of the proposed method. The empirical risk estimator according to Eq.(6) can be rewritten as:

$$\hat{R}_{sp}(f) = \frac{1}{n} \sum_{i=1}^n \sum_{j=1}^L \left(w_i^j \ell_i^j + \bar{w}_i^j \bar{\ell}_i^j \right), \quad (17)$$

where $w_i^j = \frac{d_i^j}{p(y^{\gamma_i}=1|\mathbf{x}_i)_c}$ and $\bar{w}_i^j = \frac{1-d_i^j}{p(y^{\gamma_i}=1|\mathbf{x}_i)_c}$. Then the loss function \mathcal{L}_{sp} is

$$\mathcal{L}_{sp} = \sum_{j=1}^L \left(w_i^j \ell_i^j + \bar{w}_i^j \bar{\ell}_i^j \right). \quad (18)$$

Table 1: Predictive performance of each comparing approach (mean \pm std) in terms of *Average precision* \uparrow . The best performance (the larger the better) is shown in bold face.

Datasets	SMILE	AN	AN-LS	WAN	ROLE	GLOCAL	MLML	D2ML
CAL500	0.401\pm0.011	0.382 \pm 0.044	0.253 \pm 0.031	0.393 \pm 0.011	0.288 \pm 0.008	0.227 \pm 0.002	0.233 \pm 0.000	0.223 \pm 0.001
image	0.784\pm0.044	0.613 \pm 0.081	0.621 \pm 0.073	0.685 \pm 0.058	0.696 \pm 0.039	0.771 \pm 0.003	0.652 \pm 0.001	0.274 \pm 0.003
scene	0.841\pm0.070	0.740 \pm 0.127	0.741 \pm 0.117	0.801 \pm 0.020	0.717 \pm 0.067	0.825 \pm 0.001	0.814 \pm 0.000	0.285 \pm 0.002
yeast	0.758\pm0.003	0.755 \pm 0.003	0.753 \pm 0.003	0.757 \pm 0.003	0.753 \pm 0.003	0.646 \pm 0.002	0.456 \pm 0.002	0.323 \pm 0.001
corel5k	0.303\pm0.007	0.299 \pm 0.005	0.272 \pm 0.005	0.302 \pm 0.004	0.215 \pm 0.011	0.218 \pm 0.001	0.072 \pm 0.001	0.028 \pm 0.001
rev1-s1	0.616\pm0.001	0.604 \pm 0.004	0.581 \pm 0.002	0.610 \pm 0.005	0.570 \pm 0.004	0.229 \pm 0.000	0.221 \pm 0.003	0.053 \pm 0.001
corel16k-s1	0.344\pm0.003	0.337 \pm 0.003	0.316 \pm 0.002	0.344 \pm 0.003	0.288 \pm 0.004	0.029 \pm 0.001	0.081 \pm 0.001	0.029 \pm 0.004
delicious	0.319 \pm 0.001	0.297 \pm 0.009	0.193 \pm 0.005	0.320\pm0.001	0.199 \pm 0.004	0.027 \pm 0.001	0.086 \pm 0.001	0.028 \pm 0.001
iaprtc12	0.314\pm0.003	0.292 \pm 0.008	0.244 \pm 0.008	0.266 \pm 0.006	0.243 \pm 0.005	0.035 \pm 0.002	0.126 \pm 0.001	0.026 \pm 0.001
espgame	0.259\pm0.003	0.248 \pm 0.002	0.208 \pm 0.003	0.259 \pm 0.002	0.216 \pm 0.004	0.038 \pm 0.000	0.086 \pm 0.002	0.038 \pm 0.001
mirflickr	0.635\pm0.004	0.629 \pm 0.003	0.604 \pm 0.004	0.611 \pm 0.004	0.545 \pm 0.019	0.476 \pm 0.000	0.253 \pm 0.003	0.132 \pm 0.002
tmc2007	0.820\pm0.002	0.815 \pm 0.003	0.802 \pm 0.003	0.815 \pm 0.001	0.798 \pm 0.005	0.649 \pm 0.000	0.415 \pm 0.000	0.161 \pm 0.001

We define a function space as:

$$\mathcal{G}_{sp} = \left\{ (\mathbf{x}, y) \mapsto \sum_{j=1}^L (w^j \ell^j + \bar{w}^j \bar{\ell}^j) \mid f \in \mathcal{F} \right\}, \quad (19)$$

and denote the expected Rademacher complexity [1] of \mathcal{G}_{sp} as:

$$\tilde{\mathfrak{R}}_n(\mathcal{G}_{sp}) = \mathbb{E}_{\mathbf{x}, y, \boldsymbol{\sigma}} \left[\sup_{g \in \mathcal{G}_{sp}} \frac{1}{n} \sum_{i=1}^n \sigma_i g(\mathbf{x}_i, y_i) \right], \quad (20)$$

where $\boldsymbol{\sigma} = \{\sigma_1, \sigma_2, \dots, \sigma_n\}$ is n Rademacher variables with σ_i independently uniform variable taking value in $\{+1, -1\}$. Then we have

Lemma 1 We suppose that the SPMLL loss function \mathcal{L}_{sp} could be bounded by M , i.e., $M = \sup_{\mathbf{x} \in \mathcal{X}, f \in \mathcal{F}, y \in \mathcal{Y}} \mathcal{L}_{sp}(f(\mathbf{x}), y)$, and for any $\delta > 0$, with probability at least $1 - \delta$, then we have

$$\sup_{f \in \mathcal{F}} \left| R_{sp}(f) - \hat{R}_{sp}(f) \right| \leq 2\tilde{\mathfrak{R}}_n(\mathcal{G}_{sp}) + \frac{M}{2} \sqrt{\frac{\log \frac{2}{\delta}}{2n}}.$$

The proof of Lemma 1 could be founded in Appendix C.

Lemma 2 We suppose that the loss function $\ell(f(\mathbf{x}), y)$ and $\bar{\ell}(f(\mathbf{x}), y)$ are ρ^+ -Lipschitz and ρ^- -Lipschitz with respect to $f(\mathbf{x})$ ($0 < \rho^+ < \infty$ and $0 < \rho^- < \infty$) for all $y \in \mathcal{Y}$, respectively, and w^j and \bar{w}^j are both bounded in $[0, \kappa]$. Then, we have

$$\tilde{\mathfrak{R}}_n(\mathcal{G}_{sp}) \leq \sqrt{2}\kappa c(\rho^+ + \rho^-) \sum_{j=1}^c \mathfrak{R}_n(\mathcal{H}_{y_j}),$$

where $\mathcal{H}_y = \{h : \mathbf{x} \mapsto f_y(\mathbf{x}) \mid f \in \mathcal{F}\}$ and $\mathfrak{R}_n(\mathcal{H}_y) = \mathbb{E}_{\mathbf{x}, \boldsymbol{\sigma}} \left[\sup_{h \in \mathcal{H}_y} \frac{1}{n} \sum_{i=1}^n h(\mathbf{x}_i) \right]$.

The proof of Lemma 2 could be founded in Appendix D.

Based one Lemma 1 and 2, we could obtain the following theorem:

Theorem 1 Assume the loss function $\ell(f(\mathbf{x}), y)$ and $\bar{\ell}(f(\mathbf{x}), y)$ are ρ^+ -Lipschitz and ρ^- -Lipschitz with respect to $f(\mathbf{x})$ ($0 < \rho^+ < \infty$ and $0 < \rho^- < \infty$) for all $y \in \mathcal{Y}$ and the loss function \mathcal{L}_{sp} are bounded by M , i.e., $M = \sup_{\mathbf{x} \in \mathcal{X}, f \in \mathcal{F}, y \in \mathcal{Y}} \mathcal{L}_{sp}(f(\mathbf{x}), y)$, with probability at least $1 - \delta$,

$$R(\hat{f}_{sp}) - R(f^*) \leq 4\sqrt{2}\kappa c(\rho^+ + \rho^-) \sum_{j=1}^c \mathfrak{R}_n(\mathcal{H}_y) + M \sqrt{\frac{\log \frac{2}{\delta}}{2n}}.$$

Here, $\hat{f}_{sp} = \min_{f \in \mathcal{F}} \hat{R}_{sp}(f)$ and $f^* = \min_{f \in \mathcal{F}} R(f)$ are the empirical risk minimizer and the true risk minimizer, respectively. The proof could be founded in Appendix E. Theorem 1 shows that f_{sp} would converge to f^* as $n \rightarrow \infty$ and $\mathfrak{R}_n(\mathcal{H}_y) \rightarrow 0$.

Table 2: Predictive performance of each comparing approach (mean \pm std) in terms of *One-error* \downarrow . The best performance (the smaller the better) is shown in bold face.

Datasets	SMILE	AN	AN-LS	WAN	ROLE	GLOCAL	MLML	D2ML
CAL500	0.358 \pm 0.156	0.325\pm0.134	0.627 \pm 0.188	0.420 \pm 0.152	0.557 \pm 0.034	0.843 \pm 0.011	0.839 \pm 0.032	0.833 \pm 0.003
image	0.350 \pm 0.046	0.597 \pm 0.102	0.577 \pm 0.095	0.516 \pm 0.090	0.488 \pm 0.055	0.365 \pm 0.012	0.200\pm0.023	0.600 \pm 0.019
scene	0.278 \pm 0.112	0.417 \pm 0.152	0.412 \pm 0.145	0.344 \pm 0.033	0.477 \pm 0.111	0.286 \pm 0.024	0.167\pm0.011	0.667 \pm 0.023
yeast	0.236\pm0.008	0.242 \pm 0.012	0.244 \pm 0.009	0.242 \pm 0.011	0.239 \pm 0.010	0.276 \pm 0.032	0.285 \pm 0.003	0.500 \pm 0.022
corel5k	0.648\pm0.008	0.685 \pm 0.019	0.674 \pm 0.013	0.656 \pm 0.013	0.696 \pm 0.022	0.764 \pm 0.011	0.947 \pm 0.005	0.987 \pm 0.003
rev1-s1	0.438\pm0.007	0.445 \pm 0.011	0.467 \pm 0.008	0.449 \pm 0.011	0.464 \pm 0.003	0.810 \pm 0.029	0.782 \pm 0.002	0.941 \pm 0.004
corel16k-s1	0.641\pm0.008	0.655 \pm 0.005	0.666 \pm 0.007	0.642 \pm 0.009	0.667 \pm 0.009	0.989 \pm 0.003	0.830 \pm 0.001	0.987 \pm 0.003
delicious	0.410 \pm 0.005	0.454 \pm 0.026	0.516 \pm 0.021	0.405\pm0.007	0.498 \pm 0.012	0.996 \pm 0.003	0.804 \pm 0.011	0.967 \pm 0.003
iaprtc12	0.579\pm0.022	0.604 \pm 0.022	0.618 \pm 0.017	0.662 \pm 0.015	0.659 \pm 0.016	0.997 \pm 0.000	0.605 \pm 0.012	0.897 \pm 0.006
espgame	0.662\pm0.007	0.686 \pm 0.012	0.702 \pm 0.011	0.673 \pm 0.008	0.707 \pm 0.009	0.995 \pm 0.000	0.699 \pm 0.003	0.734 \pm 0.004
mirflickr	0.335\pm0.013	0.343 \pm 0.017	0.343 \pm 0.006	0.385 \pm 0.009	0.497 \pm 0.030	0.670 \pm 0.054	0.447 \pm 0.011	0.816 \pm 0.007
tmc2007	0.204\pm0.003	0.215 \pm 0.003	0.221 \pm 0.006	0.220 \pm 0.003	0.225 \pm 0.004	0.313 \pm 0.001	0.227 \pm 0.002	0.409 \pm 0.008

Table 3: Summary of the Wilcoxon signed-ranks test for SMILE against other comparing approaches at 0.05 significance level. The p -values are shown in the brackets.

SMILE against	AN	AN-LS	WAN	ROLE	GLOCAL	MLML	D2ML
<i>Average precision</i>	win[0.0005]	win[0.0005]	win[0.0092]	win[0.0005]	win[0.0005]	win[0.0005]	win[0.0005]
<i>One-error</i>	win[0.0122]	win[0.0005]	win[0.0015]	win[0.0005]	win[0.0005]	win[0.0342]	win[0.0005]
<i>Ranking loss</i>	win[0.0269]	win[0.0005]	tie[0.1533]	win[0.0005]	win[0.0005]	win[0.0024]	win[0.0005]
<i>Hamming loss</i>	win[0.0277]	win[0.0178]	win[0.0005]	win[0.0277]	win[0.0277]	win[0.0277]	win[0.0077]
<i>Coverage</i>	win[0.0425]	win[0.0005]	tie[0.1819]	win[0.0005]	win[0.0005]	win[0.0024]	win[0.0015]

5 Experiments

5.1 Experimental Configurations

In the experiments, we adopt twelve widely-used MLL datasets [13], which cover a broad range of cases with diversified multi-label properties. To evaluate the performance of SPMLL methods, we generate the single positive training data by randomly selecting one positive label to keep for each training example in the MLL datasets. For each dataset, we run the comparing methods with 80%/10%/10% train/validation/test split. The validation and test sets are always fully labeled. The detailed descriptions of these datasets are provided in Appendix F. Five popular multi-label metrics *Ranking loss*, *Hamming loss*, *One-error*, *Coverage*, and *Average precision* [46] are employed for performance evaluation. Furthermore, for *Average precision*, the *larger* the values the better the performance. While for the other four metrics, the *smaller* the values the better the performance.

In this paper, SMILE is compared against four well-established SPMLL approaches including 1) AN [5] which assumes unobserved labels are negative and employs binary entropy loss for the training examples with the modified labels, 2) AN-LS [5] which assumes unobserved labels are negative and employs label smoothing [28] to reduce the impact of the incorrect labels (i.e. those labels incorrectly assumed to be negative), 3) WAN [5] which reduces the impact of false negatives by employing the down-weight terms in the loss corresponding to negative labels, and 4) ROLE [5] which online estimates of the unobserved labels throughout training and encourages the classifier predictions to match the estimated labels via binary entropy loss.

As SPMLL could be regarded as the hardest version of MLL with missing labels, three well-established approaches of MLL with missing labels (also termed as MLL with partial labels) are adopted as the comparing approaches including 1) GLOCAL [47] which exploits global and local label correlations simultaneously via learning a latent label representation in the missing label cases, 2) MLML [34] which recovers the full label assignment for each sample by enforcing consistency with available label assignments and smoothness of labels, and 3) D2ML [24] which utilizes both local low-rank label structures and label discriminant information for learning from missing labels.

For all the DNN-based approaches (AN, AN-LS, WAN, ROLE and SMILE), we adopt three-layer MLP as the predictive model for fair comparisons and use the Adam optimizer [17]. The mini-batch size and the number of epochs are set to 16 and 25, respectively. The learning rate and weight decay are selected from $\{10^{-4}, 10^{-3}, 10^{-2}\}$ with a validation set. Other hyper-parameters for all the comparing methods are also selected based on the validation. All the comparing methods run 5 trials (with 80%/10%/10% train/validation/test split) on each dataset.

Table 4: Predictive performance of SMILE and its variant (mean \pm std) in terms of *Average precision*, *One-error*, and *Ranking loss*.

Datasets	Average precision \uparrow		One-error \downarrow		Ranking loss \downarrow	
	SMILE	SMILE-SI	SMILE	SMILE-SI	SMILE	SMILE-SI
CAL500	0.401 \pm 0.011	0.409\pm0.000	0.358 \pm 0.156	0.343\pm0.010	0.239\pm0.010	0.244 \pm 0.000
image	0.784\pm0.044	0.547 \pm 0.022	0.350\pm0.046	0.675 \pm 0.035	0.170\pm0.055	0.428 \pm 0.005
scene	0.841\pm0.070	0.711 \pm 0.057	0.278\pm0.112	0.483 \pm 0.093	0.086\pm0.045	0.168 \pm 0.037
yeast	0.758\pm0.003	0.738 \pm 0.002	0.236\pm0.008	0.246 \pm 0.006	0.161\pm0.003	0.176 \pm 0.001
corel5k	0.303\pm0.007	0.302 \pm 0.003	0.648\pm0.008	0.655 \pm 0.007	0.134 \pm 0.003	0.116\pm0.000
rcv1-s1	0.616\pm0.001	0.577 \pm 0.004	0.438\pm0.007	0.477 \pm 0.015	0.042\pm0.000	0.055 \pm 0.000
corel16k-s1	0.344\pm0.003	0.336 \pm 0.001	0.641\pm0.008	0.649 \pm 0.002	0.133\pm0.001	0.140 \pm 0.000
delicious	0.319\pm0.001	0.293 \pm 0.004	0.410\pm0.005	0.434 \pm 0.023	0.126\pm0.000	0.146 \pm 0.002
iaprtc12	0.314\pm0.003	0.287 \pm 0.001	0.579\pm0.022	0.607 \pm 0.015	0.115\pm0.002	0.143 \pm 0.002
espgame	0.259\pm0.003	0.249 \pm 0.003	0.662\pm0.007	0.675 \pm 0.002	0.158\pm0.001	0.170 \pm 0.002
mirflickr	0.635\pm0.004	0.628 \pm 0.001	0.335\pm0.013	0.349 \pm 0.012	0.117\pm0.002	0.122 \pm 0.002
tmc2007	0.820\pm0.002	0.814 \pm 0.001	0.204\pm0.003	0.210 \pm 0.003	0.049 \pm 0.001	0.048\pm0.000

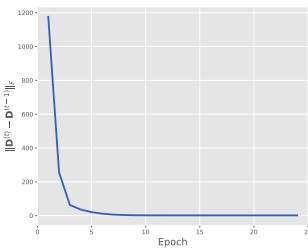
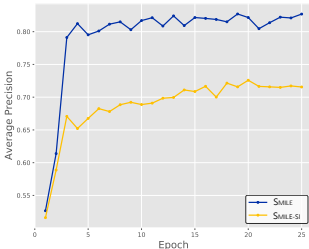


Figure 2: *Average precision*. Figure 3: Convergence of \mathbf{D} .

Table 5: Wilcoxon signed ranks test (at 0.05 significance level).

Evaluation metric	SMILE against SMILE-SI	
	performance	p -value
<i>Average precision</i>	win	0.0049
<i>One-error</i>	win	0.0092
<i>Ranking loss</i>	win	0.0161
<i>Hamming loss</i>	win	0.0277
<i>Coverage</i>	win	0.0122

5.2 Experimental Results

Tables 1 and 2 report the results of all approaches on *Average precision* and *One-error*, respectively. For each evaluation metric, “ \uparrow ” indicates “the smaller the better” while “ \downarrow ” indicates “the larger the better”. The results on other metrics are similar and could be seen in Appendix F. In addition, Wilcoxon signed-ranks test [6] is employed to show whether SMILE has a significant performance than other comparing approaches. Table 3 reports the p -values for the corresponding tests and the statistical test results at 0.05 significance level.

Table 3 shows that SMILE achieves superior performance against all the comparing approaches on all evaluation metrics (except on *Ranking loss* and *Coverage* where SMILE achieves comparable performance against WAN). The superior performance of SMILE provides a strong evidence for the effectiveness of risk-consistent estimator for SPMLL. Tables 1 and 2 show that the performance advantage of SMILE over comparing approaches is stable under varying the number of class labels. In summary, these experimental results clearly validate the effectiveness of SMILE.

5.3 Further Analysis

To show the helpfulness of label enhancement to SMILE, a vanilla variant of SMILE (named SMILE-SI) is adopted. Here, label enhancement is replaced by approximating d_i^j with the confidence of the current model $f_j(x_i)$, which is a widely-used technique [9, 22] to approximate the soft label in weakly supervised learning. Table 4 reports detailed experimental results in terms of *Average precision*, *One-error*, and *Ranking loss*, respectively. The detailed experimental results in terms of other metrics are reported in Appendix F. Besides, the performance of each approach with the number of epochs on *scene* is shown in Figure 2. Wilcoxon signed-ranks test [6] in Table 5 shows that SMILE achieves superior performance against SMILE-SI on all evaluation metrics, which clearly validates the usefulness of label enhancement. Figure 3 illustrates the estimated \mathbf{D} converges with the number of epochs on *delicious*, which shows that the estimated soft label could converge efficiently.

6 Conclusion

In this paper, we study single-positive multi-label learning and propose a novel approach SMILE. We derive an unbiased risk estimator, which suggests that one positive label of each instance is sufficient to train predictive models for multi-label learning, and design a benchmark solution via estimating the soft label corresponding to each example in a label enhancement process. The effectiveness of the proposed method is validated on twelve corrupted MLL datasets.

References

- [1] Peter L Bartlett and Shahar Mendelson. Rademacher and gaussian complexities: Risk bounds and structural results. *Journal of Machine Learning Research*, 3(Nov):463–482, 2002.
- [2] Matthew R Boutell, Jiebo Luo, Xipeng Shen, and Christopher M Brown. Learning multi-label scene classification. *Pattern Recognition*, 37(9):1757–1771, 2004.
- [3] Di Chen, Yexiang Xue, Shuo Chen, Daniel Fink, and Carla Gomes. Deep multi-species embedding. *arXiv preprint arXiv:1609.09353*, 2016.
- [4] Zhao-Min Chen, Xiu-Shen Wei, Peng Wang, and Yanwen Guo. Multi-label image recognition with graph convolutional networks. In *Proceedings of the IEEE/CVF Conference on Computer Vision and Pattern Recognition*, pages 5177–5186, 2019.
- [5] Elijah Cole, Oisín Mac Aodha, Titouan Llorient, Pietro Perona, Dan Morris, and Nebojsa Jojic. Multi-label learning from single positive labels. In *Proceedings of the IEEE/CVF Conference on Computer Vision and Pattern Recognition*, pages 933–942, 2021.
- [6] Janez Demšar. Statistical comparisons of classifiers over multiple data sets. *Journal of Machine Learning Research*, 7(Jan):1–30, 2006.
- [7] Thibaut Durand, Nazanin Mehrasa, and Greg Mori. Learning a deep convnet for multi-label classification with partial labels. In *Proceedings of the IEEE/CVF Conference on Computer Vision and Pattern Recognition*, pages 647–657, 2019.
- [8] André Elisseeff and Jason Weston. A kernel method for multi-labelled classification. In *Advances in Neural Information Processing Systems 14 (NIPS 2002)*, pages 681–687, Vancouver, British Columbia, Canada, 2002.
- [9] Lei Feng, Jiaqi Lv, Bo Han, Miao Xu, Gang Niu, Xin Geng, Bo An, and Masashi Sugiyama. Provably consistent partial-label learning. *Advances in Neural Information Processing Systems*, 2020.
- [10] Michael Figurnov, Shakir Mohamed, and Andriy Mnih. Implicit reparameterization gradients. *Advances in Neural Information Processing Systems*, 2018.
- [11] Johannes Fürnkranz, Eyke Hüllermeier, Eneldo Loza Mencía, and Klaus Brinker. Multilabel classification via calibrated label ranking. *Machine Learning*, 73(2):133–153, 2008.
- [12] Andrew B. Goldberg, Xiaojin Zhu, Ben Recht, Jun-Ming Xu, and Robert D. Nowak. Transduction with matrix completion: Three birds with one stone. In *Advances in Neural Information Processing Systems 23*, pages 757–765. Curran Associates, Inc., 2010.
- [13] Jun-Yi Hang and Min-Ling Zhang. Collaborative learning of label semantics and deep label-specific features for multi-label classification. *IEEE Transactions on Pattern Analysis and Machine Intelligence*, 2021.
- [14] Thomas Hartvigsen, Cansu Sen, Xiangnan Kong, and Elke Rundensteiner. Recurrent halting chain for early multi-label classification. In *Proceedings of the 26th ACM SIGKDD International Conference on Knowledge Discovery & Data Mining*, pages 1382–1392, 2020.
- [15] Jun Huang, Guorong Li, Qingming Huang, and Xindong Wu. Learning label-specific features and class-dependent labels for multi-label classification. *IEEE transactions on knowledge and data engineering*, 28(12):3309–3323, 2016.
- [16] Dat Huynh and Ehsan Elhamifar. Interactive multi-label cnn learning with partial labels. In *Proceedings of the IEEE/CVF Conference on Computer Vision and Pattern Recognition*, pages 9423–9432, 2020.

- [17] Diederik P. Kingma and Jimmy Ba. Adam: A method for stochastic optimization. In *3rd International Conference on Learning Representations, 2015, San Diego, CA*, 2015.
- [18] Diederik P Kingma and Max Welling. Auto-encoding variational bayes. In *International Conference on Learning Representations*, Banff, AB, Canada, 2014.
- [19] Thomas N Kipf and Max Welling. Variational graph auto-encoders. *arXiv preprint arXiv:1611.07308*, 2016.
- [20] Jack Lanchantin, Tianlu Wang, Vicente Ordonez, and Yanjun Qi. General multi-label image classification with transformers. In *Proceedings of the IEEE/CVF Conference on Computer Vision and Pattern Recognition*, pages 16478–16488, 2021.
- [21] Hung-Yi Lo, Ju-Chiang Wang, Hsin-Min Wang, and Shou-De Lin. Cost-sensitive multi-label learning for audio tag annotation and retrieval. *IEEE Transactions on Multimedia*, 13(3):518–529, 2011.
- [22] Jiaqi Lv, Miao Xu, Lei Feng, Gang Niu, Xin Geng, and Masashi Sugiyama. Progressive identification of true labels for partial-label learning. In *International Conference on Machine Learning*, pages 6500–6510. PMLR, 2020.
- [23] Jianghong Ma and Tommy WS Chow. Topic-based instance and feature selection in multilabel classification. *IEEE Transactions on Neural Networks and Learning Systems*, 2020.
- [24] Zhongchen Ma and Songcan Chen. Expand globally, shrink locally: Discriminant multi-label learning with missing labels. *Pattern Recognition*, 111:107675, 2021.
- [25] Mehryar Mohri, Afshin Rostamizadeh, and Ameet Talwalkar. *Foundations of machine learning*. MIT press, 2018.
- [26] Jesse Read, Bernhard Pfahringer, Geoff Holmes, and Eibe Frank. Classifier chains for multi-label classification. *Machine Learning*, 85(3):333, 2011.
- [27] Timothy N Rubin, America Chambers, Padhraic Smyth, and Mark Steyvers. Statistical topic models for multi-label document classification. *Machine learning*, 88(1-2):157–208, 2012.
- [28] Christian Szegedy, Vincent Vanhoucke, Sergey Ioffe, Jon Shlens, and Zbigniew Wojna. Rethinking the inception architecture for computer vision. In *Proceedings of the IEEE conference on computer vision and pattern recognition*, pages 2818–2826, 2016.
- [29] Pingjie Tang, Meng Jiang, Bryan Ning Xia, Jed W Pitera, Jeffrey Welser, and Nitesh V Chawla. Multi-label patent categorization with non-local attention-based graph convolutional network. In *Proceedings of the AAAI Conference on Artificial Intelligence*, volume 34, pages 9024–9031, 2020.
- [30] Grigorios Tsoumakas and Ioannis Katakis. Multi-label classification: An overview. *International Journal of Data Warehousing and Mining*, 3(3):1–13, 2006.
- [31] Grigorios Tsoumakas, Ioannis Katakis, and Ioannis Vlahavas. Mining multi-label data. In *Data mining and knowledge discovery handbook*, pages 667–685. Springer, 2009.
- [32] Grigorios Tsoumakas, Ioannis Katakis, and Ioannis Vlahavas. Random k-labelsets for multilabel classification. *IEEE Transactions on Knowledge and Data Engineering*, 23(7):1079–1089, 2011.
- [33] Alexis Vallet and Hiroyasu Sakamoto. A multi-label convolutional neural network for automatic image annotation. *Journal of information processing*, 23(6):767–775, 2015.
- [34] Baoyuan Wu, Zhilei Liu, Shangfei Wang, Bao-Gang Hu, and Qiang Ji. Multi-label learning with missing labels. In *2014 22nd International Conference on Pattern Recognition*, pages 1964–1968. IEEE, 2014.
- [35] Bin Wu, Erheng Zhong, Andrew Horner, and Qiang Yang. Music emotion recognition by multi-label multi-layer multi-instance multi-view learning. In *Proceedings of the 22nd ACM international conference on Multimedia*, pages 117–126, 2014.
- [36] Ning Xu, Yun-Peng Liu, and Xin Geng. Label enhancement for label distribution learning. *IEEE Transactions on Knowledge and Data Engineering*, 33(4):1632 – 1643, 2021.
- [37] Ning Xu, Congyu Qiao, Xin Geng, and Min-Ling Zhang. Instance-dependent partial label learning. *Advances in Neural Information Processing Systems*, 34, 2021.

- [38] Ning Xu, Jun Shu, Yun-Peng Liu, and Xin Geng. Variational label enhancement. In *Proceedings of the International Conference on Machine Learning*, pages 10597–10606, Vienna, Austria, 2020.
- [39] Ning Xu, Jun Shu, Ren-Yi Zheng, Xin Geng, Deyu Meng, and Min-Ling Zhang. Variational label enhancement. *IEEE Transactions on Pattern Analysis and Machine Intelligence*, page in press, 2021.
- [40] Renchun You, Zhiyao Guo, Lei Cui, Xiang Long, Yingze Bao, and Shilei Wen. Cross-modality attention with semantic graph embedding for multi-label classification. In *Proceedings of the AAAI Conference on Artificial Intelligence*, volume 34, pages 12709–12716, 2020.
- [41] Hsiang-Fu Yu, Prateek Jain, Purushottam Kar, and Inderjit Dhillon. Large-scale multi-label learning with missing labels. In *International conference on machine learning*, pages 593–601. PMLR, 2014.
- [42] Ze-Bang Yu and Min-Ling Zhang. Multi-label classification with label-specific feature generation: A wrapped approach. *IEEE Transactions on Pattern Analysis and Machine Intelligence*, 2021.
- [43] Chiyuan Zhang, Samy Bengio, Moritz Hardt, Benjamin Recht, and Oriol Vinyals. Understanding deep learning requires rethinking generalization. In *5th International Conference on Learning Representations*, Toulon, France.
- [44] Jing Zhang and Xindong Wu. Multi-label inference for crowdsourcing. In *Proceedings of the 24th ACM SIGKDD International Conference on Knowledge Discovery & Data Mining*, pages 2738–2747, 2018.
- [45] Min-Ling Zhang and Zhi-Hua Zhou. Ml-knn: A lazy learning approach to multi-label learning. *Pattern Recognition*, 40(7):2038–2048, 2007.
- [46] Min-Ling Zhang and Zhi-Hua Zhou. A review on multi-label learning algorithms. *IEEE Transactions on Knowledge and Data Engineering*, 26(8):1819–1837, 2014.
- [47] Yue Zhu, James T Kwok, and Zhi-Hua Zhou. Multi-label learning with global and local label correlation. *IEEE Transactions on Knowledge and Data Engineering*, 30(6):1081–1094, 2017.

A Calculation Details of Eq. (4)

$$\begin{aligned}
& \sum_{Y \in \mathcal{C}} \mathcal{L}(f(\mathbf{x}), Y) p(Y|\mathbf{x}) \\
&= \sum_{Y \in \mathcal{C}} \sum_{j \in Y} \ell^j p(Y|\mathbf{x}) + \sum_{Y \in \mathcal{C}} \sum_{j \notin Y} \bar{\ell}^j p(Y|\mathbf{x}) \\
&= \sum_{j=1}^c \ell^j \sum_{Y \in \mathcal{C}_j} p(Y|\mathbf{x}) + \sum_{j=1}^c \bar{\ell}^j \sum_{Y \in \tilde{\mathcal{C}}_j} p(Y|\mathbf{x}) \\
&= \sum_{j=1}^c p(y^j = 1|\mathbf{x}) \ell^j \sum_{Y \in \mathcal{C}_j} \prod_{k \in Y, k \neq j} p(y^k = 1|\mathbf{x}) \prod_{k \notin Y} (1 - p(y^k = 1|\mathbf{x})) + \\
&\quad \sum_{j=1}^c (1 - p(y^j = 1|\mathbf{x})) \bar{\ell}^j \sum_{Y \in \tilde{\mathcal{C}}_j} \prod_{k \in Y} p(y^k = 1|\mathbf{x}) \prod_{k \notin Y, k \neq j} (1 - p(y^k = 1|\mathbf{x})) \\
&= \sum_{j=1}^c p(y^j = 1|\mathbf{x}) \ell^j + (1 - p(y^j = 1|\mathbf{x})) \bar{\ell}^j \\
&= \sum_{j=1}^c d^j \ell^j + (1 - d^j) \bar{\ell}^j.
\end{aligned} \tag{21}$$

where $d^j = p(y^j = 1|\mathbf{x})$, \mathcal{C}_j denotes the subset of \mathcal{C} which contains label j and $\tilde{\mathcal{C}}_j$ denotes the subset of \mathcal{C} without label j .

B Calculation Details of Eq. (4)

$$\log p(\mathbf{L}, \mathbf{X}, \mathbf{A}) = \log \mathbf{p}(\mathbf{D}, \mathbf{Z}, \mathbf{L}, \mathbf{X}, \mathbf{A}) - \log \mathbf{p}(\mathbf{D}, \mathbf{Z}|\mathbf{L}, \mathbf{X}, \mathbf{A}). \tag{22}$$

Multiply both sides by $q_w(\mathbf{Z}, \mathbf{D}|\mathbf{L}, \mathbf{X}, \mathbf{A})$, and for \mathbf{D} and \mathbf{Z} integral:

$$\begin{aligned}
& \int_{\mathbf{Z}, \mathbf{D}} q_w(\mathbf{Z}, \mathbf{D} | \mathbf{L}, \mathbf{X}, \mathbf{A}) \log \mathbf{p}(\mathbf{L}, \mathbf{X}, \mathbf{A}) d\mathbf{Z}d\mathbf{D} \\
&= \int_{\mathbf{Z}, \mathbf{D}} q_w(\mathbf{Z}, \mathbf{D} | \mathbf{L}, \mathbf{X}, \mathbf{A}) (\log \mathbf{p}(\mathbf{D}, \mathbf{Z}, \mathbf{L}, \mathbf{X}, \mathbf{A}) - \log \mathbf{p}(\mathbf{D}, \mathbf{Z} | \mathbf{L}, \mathbf{X}, \mathbf{A})) d\mathbf{Z}d\mathbf{D}.
\end{aligned} \tag{23}$$

On the left side, $\log p(\mathbf{L}, \mathbf{X}, \mathbf{A})$ is independent of \mathbf{D} and \mathbf{Z} :

$$\begin{aligned}
& \log p(\mathbf{L}, \mathbf{X}, \mathbf{A}) = \int_{\mathbf{Z}, \mathbf{D}} q_w(\mathbf{Z}, \mathbf{D} | \mathbf{L}, \mathbf{X}, \mathbf{A}) (\log \mathbf{p}(\mathbf{Z}, \mathbf{D}, \mathbf{L}, \mathbf{X}, \mathbf{A}) \\
&\quad - \log \mathbf{p}(\mathbf{Z}, \mathbf{D} | \mathbf{L}, \mathbf{X}, \mathbf{A})) d\mathbf{Z}d\mathbf{D} \\
&= \int_{\mathbf{Z}, \mathbf{D}} q_w(\mathbf{Z}, \mathbf{D} | \mathbf{L}, \mathbf{X}, \mathbf{A}) \left(\log \frac{\mathbf{p}(\mathbf{Z}, \mathbf{D}, \mathbf{L}, \mathbf{X}, \mathbf{A})}{q_w(\mathbf{Z}, \mathbf{D} | \mathbf{L}, \mathbf{X}, \mathbf{A})} - \log \frac{\mathbf{p}(\mathbf{Z}, \mathbf{D} | \mathbf{L}, \mathbf{X}, \mathbf{A})}{q_w(\mathbf{Z}, \mathbf{D} | \mathbf{L}, \mathbf{X}, \mathbf{A})} \right) d\mathbf{Z}d\mathbf{D} \\
&= \int_{\mathbf{Z}, \mathbf{D}} q_w(\mathbf{Z}, \mathbf{D} | \mathbf{L}, \mathbf{X}, \mathbf{A}) \log \frac{\mathbf{p}(\mathbf{Z}, \mathbf{D}, \mathbf{L}, \mathbf{X}, \mathbf{A})}{q_w(\mathbf{Z}, \mathbf{D} | \mathbf{L}, \mathbf{X}, \mathbf{A})} d\mathbf{Z}d\mathbf{D} \\
&\quad + \text{KL}[q_w(\mathbf{Z}, \mathbf{D} | \mathbf{L}, \mathbf{X}, \mathbf{A}) || \mathbf{p}(\mathbf{Z}, \mathbf{D} | \mathbf{L}, \mathbf{X}, \mathbf{A})].
\end{aligned} \tag{24}$$

On the right side, the first term is called ELBO:

$$\mathcal{L}_{ELBO} = \int_{\mathbf{Z}, \mathbf{D}} q_w(\mathbf{Z}, \mathbf{D} | \mathbf{L}, \mathbf{X}, \mathbf{A}) \log \frac{\mathbf{p}(\mathbf{Z}, \mathbf{D}, \mathbf{L}, \mathbf{X}, \mathbf{A})}{q_w(\mathbf{Z}, \mathbf{D} | \mathbf{L}, \mathbf{X}, \mathbf{A})} d\mathbf{Z}d\mathbf{D}. \tag{25}$$

Then we have:

$$\log p(\mathbf{L}, \mathbf{X}, \mathbf{A}) = \mathcal{L}_{ELBO} + \text{KL}[q_w(\mathbf{Z}, \mathbf{D} | \mathbf{L}, \mathbf{X}, \mathbf{A}) || \mathbf{p}(\mathbf{Z}, \mathbf{D} | \mathbf{L}, \mathbf{X}, \mathbf{A})]. \tag{26}$$

\mathcal{L}_{ELBO} can be calculated as:

$$\begin{aligned}
\mathcal{L}_{ELBO} &= \int_{\mathbf{Z}, \mathbf{D}} q_{\mathbf{w}}(\mathbf{Z}, \mathbf{D} \mid \mathbf{L}, \mathbf{X}, \mathbf{A}) \log \frac{p(\mathbf{Z}, \mathbf{D}, \mathbf{L}, \mathbf{X}, \mathbf{A})}{q_{\mathbf{w}}(\mathbf{Z}, \mathbf{D} \mid \mathbf{L}, \mathbf{X}, \mathbf{A})} d\mathbf{Z}d\mathbf{D} \\
&= \mathbb{E}_{q_{\mathbf{w}}(\mathbf{Z}, \mathbf{D} \mid \mathbf{L}, \mathbf{X}, \mathbf{A})} \left[\log \frac{p(\mathbf{Z}, \mathbf{D}, \mathbf{L}, \mathbf{X}, \mathbf{A})}{q_{\mathbf{w}}(\mathbf{Z}, \mathbf{D} \mid \mathbf{L}, \mathbf{X}, \mathbf{A})} \right] \\
&= \mathbb{E}_{q_{\mathbf{w}}(\mathbf{Z}, \mathbf{D} \mid \mathbf{L}, \mathbf{X}, \mathbf{A})} \left[\log \frac{p(\mathbf{Z})p(\mathbf{D})p(\mathbf{L}, \mathbf{X}, \mathbf{A} \mid \mathbf{Z}, \mathbf{D})}{q_{\mathbf{w}_1}(\mathbf{D} \mid \mathbf{L}, \mathbf{X}, \mathbf{A})q_{\mathbf{w}_2}(\mathbf{Z} \mid \mathbf{D}, \mathbf{X})} \right] \\
&= \mathbb{E}_{q_{\mathbf{w}}(\mathbf{Z}, \mathbf{D} \mid \mathbf{L}, \mathbf{X}, \mathbf{A})} [\log p(\mathbf{L}, \mathbf{X}, \mathbf{A} \mid \mathbf{Z}, \mathbf{D})] \\
&\quad + \mathbb{E}_{q_{\mathbf{w}}(\mathbf{Z}, \mathbf{D} \mid \mathbf{L}, \mathbf{X}, \mathbf{A})} \left[\log \frac{p(\mathbf{Z})p(\mathbf{D})}{q_{\mathbf{w}_1}(\mathbf{D} \mid \mathbf{L}, \mathbf{X}, \mathbf{A})q_{\mathbf{w}_2}(\mathbf{Z} \mid \mathbf{D}, \mathbf{X})} \right].
\end{aligned} \tag{27}$$

The first term of \mathcal{L}_{ELBO} can be calculated as:

$$\begin{aligned}
\mathbb{E}_{q_{\mathbf{w}}(\mathbf{Z}, \mathbf{D} \mid \mathbf{L}, \mathbf{X}, \mathbf{A})} [\log p(\mathbf{L}, \mathbf{X}, \mathbf{A} \mid \mathbf{Z}, \mathbf{D})] &= \mathbb{E}_{q_{\mathbf{w}}(\mathbf{Z}, \mathbf{D} \mid \mathbf{L}, \mathbf{X}, \mathbf{A})} [\log p(\mathbf{X} \mid \mathbf{Z}, \mathbf{D})] \\
&\quad + \mathbb{E}_{q_{\mathbf{w}}(\mathbf{Z}, \mathbf{D} \mid \mathbf{L}, \mathbf{X}, \mathbf{A})} [\log P(\mathbf{L} \mid \mathbf{D})] \\
&\quad + \mathbb{E}_{q_{\mathbf{w}}(\mathbf{Z}, \mathbf{D} \mid \mathbf{L}, \mathbf{X}, \mathbf{A})} [\log p(\mathbf{A} \mid \mathbf{D})].
\end{aligned} \tag{28}$$

The second term of \mathcal{L}_{ELBO} can be calculated as:

$$\begin{aligned}
&\mathbb{E}_{q_{\mathbf{w}}(\mathbf{Z}, \mathbf{D} \mid \mathbf{L}, \mathbf{X}, \mathbf{A})} [\log p(\mathbf{A} \mid \mathbf{D})] \\
&= \mathbb{E}_{q_{\mathbf{w}_1}(\mathbf{D} \mid \mathbf{L}, \mathbf{X}, \mathbf{A})} \mathbb{E}_{q_{\mathbf{w}_2}(\mathbf{Z} \mid \mathbf{D}, \mathbf{X})} \left[\log \frac{p(\mathbf{Z})p(\mathbf{D})}{q_{\mathbf{w}_1}(\mathbf{D} \mid \mathbf{L}, \mathbf{X}, \mathbf{A})q_{\mathbf{w}_2}(\mathbf{Z} \mid \mathbf{D}, \mathbf{X})} \right] \\
&= \mathbb{E}_{q_{\mathbf{w}_1}(\mathbf{D} \mid \mathbf{L}, \mathbf{X}, \mathbf{A})} \mathbb{E}_{q_{\mathbf{w}_2}(\mathbf{Z} \mid \mathbf{D}, \mathbf{X})} \left[\log \frac{p(\mathbf{D})}{q_{\mathbf{w}_1}(\mathbf{D} \mid \mathbf{L}, \mathbf{X}, \mathbf{A})} \right] \\
&\quad + \mathbb{E}_{q_{\mathbf{w}_1}(\mathbf{D} \mid \mathbf{L}, \mathbf{X}, \mathbf{A})} \mathbb{E}_{q_{\mathbf{w}_2}(\mathbf{Z} \mid \mathbf{D}, \mathbf{X})} \left[\log \frac{p(\mathbf{Z})}{q_{\mathbf{w}_2}(\mathbf{Z} \mid \mathbf{D}, \mathbf{X})} \right] \\
&= -\text{KL} [q_{\mathbf{w}_1}(\mathbf{D} \mid \mathbf{L}, \mathbf{X}, \mathbf{A}) \parallel p(\mathbf{D})] - \text{KL} [q_{\mathbf{w}_2}(\mathbf{Z} \mid \mathbf{D}, \mathbf{X}) \parallel p(\mathbf{Z})].
\end{aligned} \tag{29}$$

Then we have:

$$\begin{aligned}
\mathcal{L}_{ELBO} &= \mathbb{E}_{q_{\mathbf{w}}(\mathbf{Z}, \mathbf{D} \mid \mathbf{L}, \mathbf{X}, \mathbf{A})} [\log p(\mathbf{X} \mid \mathbf{Z}, \mathbf{D}) + \log P(\mathbf{L} \mid \mathbf{D}) + \log p(\mathbf{A} \mid \mathbf{D})] \\
&\quad - \text{KL} [q_{\mathbf{w}_1}(\mathbf{D} \mid \mathbf{L}, \mathbf{X}, \mathbf{A}) \parallel p(\mathbf{D})] - \text{KL} [q_{\mathbf{w}_2}(\mathbf{Z} \mid \mathbf{D}, \mathbf{X}) \parallel p(\mathbf{Z})].
\end{aligned} \tag{30}$$

C Proof of Lemma 1

In order to prove this lemma, we first show that the one direction $\sup_{f \in \mathcal{F}} R_{sp}(f) - \widehat{R}_{sp}(f)$ is bounded with probability at least $1 - \delta/2$, and the other direction can be similarly shown. Suppose an example (\mathbf{x}, y) is replaced by another arbitrary example (\mathbf{x}', y') , then the change of $\sup_{f \in \mathcal{F}} R_{sp}(f) - \widehat{R}_{sp}(f)$ is no greater than $M/(2n)$, the loss function \mathcal{L}_{sp} are bounded by M . By applying McDiarmid's inequality, for any $\delta > 0$, with probability at least $1 - \delta/2$,

$$\sup_{f \in \mathcal{F}} R_{sp}(f) - \widehat{R}_{sp}(f) \leq \mathbb{E} \left[\sup_{f \in \mathcal{F}} R_{sp}(f) - \widehat{R}_{sp}(f) \right] + \frac{M}{2} \sqrt{\frac{\log \frac{2}{\delta}}{2n}}. \tag{31}$$

By symmetrization, we can obtain

$$\mathbb{E} \left[\sup_{f \in \mathcal{F}} R_{sp}(f) - \widehat{R}_{sp}(f) \right] \leq 2\widetilde{\mathfrak{R}}_n(\mathcal{G}_{sp}). \tag{32}$$

By further taking into account the other side $\sup_{f \in \mathcal{F}} R_{sp}(f) - \widehat{R}_{sp}(f)$, we have for any $\delta > 0$, with probability at least $1 - \delta$,

$$\sup_{f \in \mathcal{F}} \left| R_{sp}(f) - \widehat{R}_{sp}(f) \right| \leq 2\widetilde{\mathfrak{R}}_n(\mathcal{G}_{sp}) + \frac{M}{2} \sqrt{\frac{\log \frac{2}{\delta}}{2n}}. \tag{33}$$

Table 6: Characteristics of the experimental datasets.

Dataset	$ \mathcal{S} $	$\dim(\mathcal{S})$	$L(\mathcal{S})$	Domain
CAL500	502	68	174	Music
image	2000	294	5	Images
scene	2407	294	6	Images
yeast	2417	103	14	Biology
corel5k	5000	499	374	Images
rcv1-s1	6000	944	101	Text
corel16k-s1	13766	500	153	Images
delicious	16105	500	983	Text
iaprtc12	19627	1000	291	Images
espgame	20770	1000	268	Images
mirflickr	25000	1000	38	Images
tmc2007	28596	981	22	Text

Table 7: Predictive performance of each comparing approach (mean \pm std) in terms of *Hamming loss* \downarrow . The best performance (the smaller the better) is shown in bold face.

Datasets	SMILE	AN	AN-LS	WAN	ROLE	GLOCAL	MLML	D2ML
CAL500	0.148\pm0.000	0.148 \pm 0.000	0.149 \pm 0.001	0.296 \pm 0.007	0.148 \pm 0.000	0.148 \pm 0.000	0.148 \pm 0.000	0.148 \pm 0.000
image	0.205\pm0.008	0.216 \pm 0.012	0.213 \pm 0.014	0.321 \pm 0.050	0.214 \pm 0.019	0.211 \pm 0.004	0.227 \pm 0.005	0.712 \pm 0.018
scene	0.124\pm0.035	0.141 \pm 0.021	0.137 \pm 0.023	0.193 \pm 0.029	0.174 \pm 0.014	0.149 \pm 0.017	0.174 \pm 0.019	0.288 \pm 0.007
yeast	0.205\pm0.003	0.306 \pm 0.000	0.306 \pm 0.000	0.215 \pm 0.003	0.213 \pm 0.006	0.277 \pm 0.073	0.306 \pm 0.035	0.694 \pm 0.015
corel5k	0.010\pm0.000	0.010 \pm 0.000	0.010 \pm 0.000	0.038 \pm 0.002	0.010 \pm 0.000	0.010 \pm 0.000	0.010 \pm 0.000	0.020 \pm 0.000
rcv1-s1	0.027\pm0.000	0.028 \pm 0.000	0.028 \pm 0.000	0.047 \pm 0.004	0.028 \pm 0.000	0.029 \pm 0.000	0.029 \pm 0.000	0.917 \pm 0.000
corel16k-s1	0.019\pm0.004	0.019 \pm 0.000	0.019 \pm 0.000	0.136 \pm 0.005	0.019 \pm 0.000	0.019 \pm 0.000	0.019 \pm 0.000	0.077 \pm 0.000
delicious	0.019\pm0.001	0.019 \pm 0.000	0.019 \pm 0.000	0.075 \pm 0.007	0.019 \pm 0.000	0.019 \pm 0.000	0.019 \pm 0.000	0.326 \pm 0.000
iaprtc12	0.019\pm0.011	0.019 \pm 0.000	0.019 \pm 0.000	0.195 \pm 0.007	0.019 \pm 0.000	0.019 \pm 0.000	0.019 \pm 0.000	0.019 \pm 0.000
espgame	0.017\pm0.003	0.017 \pm 0.000	0.017 \pm 0.000	0.174 \pm 0.009	0.017 \pm 0.000	0.017 \pm 0.000	0.017 \pm 0.000	0.017 \pm 0.000
mirflickr	0.118\pm0.001	0.127 \pm 0.000	0.127 \pm 0.000	0.211 \pm 0.003	0.130 \pm 0.005	0.128 \pm 0.000	0.128 \pm 0.000	0.128 \pm 0.000
tmc2007	0.063\pm0.000	0.085 \pm 0.001	0.089 \pm 0.001	0.092 \pm 0.004	0.065 \pm 0.002	0.098 \pm 0.001	0.098 \pm 0.001	0.098 \pm 0.000

D Proof of Lemma 2

As w^j and \bar{w}^j are bounded in $[0, \kappa]$, we can obtain $\tilde{\mathfrak{R}}_n(\mathcal{G}_{spl}) \leq \kappa c (\mathfrak{R}_n(\ell \circ \mathcal{F}) + \mathfrak{R}_n(\bar{\ell} \circ \mathcal{F}))$ where $\ell \circ \mathcal{F}$ denotes $\{\ell \circ \mathcal{F} | f \in \mathcal{F}\}$ and $\bar{\ell} \circ \mathcal{F}$ denotes $\{\bar{\ell} \circ \mathcal{F} | f \in \mathcal{F}\}$. Since $\mathcal{H}_y = \{h : \mathbf{x} \mapsto f_y(\mathbf{x}) | f \in \mathcal{F}\}$ and the loss functions $\ell(f(\mathbf{x}), y)$ and $\bar{\ell}(f(\mathbf{x}), y)$ are ρ^+ -Lipschitz and ρ^- -Lipschitz with respect to $f(\mathbf{x})$ ($0 < \rho^+ < \infty$ and $0 < \rho^- < \infty$) for all $y \in \mathcal{Y}$, by the Rademacher vector contraction inequality, we have $\mathfrak{R}_n(\ell \circ \mathcal{F}) + \mathfrak{R}_n(\bar{\ell} \circ \mathcal{F}) \leq \sqrt{2}(\rho^+ + \rho^-) \sum_{j=1}^c \mathfrak{R}_n(\mathcal{H}_y)$.

E Proof of Theorem 1

Combining Lemma 1 and 2, we have

$$\begin{aligned}
R(\hat{f}_{sp}) - R(f^*) &= R(\hat{f}_{sp}) - \hat{R}_{sp}(\hat{f}) + \hat{R}_{sp}(\hat{f}) - \hat{R}_{sp}(f^*) + \hat{R}_{sp}(f^*) - R(f^*) \\
&\leq R(\hat{f}_{sp}) - \hat{R}_{sp}(\hat{f}) + \hat{R}_{sp}(f^*) - R(f^*) \\
&\leq 2 \sup_{f \in \mathcal{F}} \left| R_{sp}(f) - \hat{R}_{sp}(f) \right| \\
&\leq 4\tilde{\mathfrak{R}}_n(\mathcal{G}_{sp}) + M \sqrt{\frac{\log \frac{2}{\delta}}{2n}} \\
&\leq 4\sqrt{2}\kappa c(\rho^+ + \rho^-) \sum_{j=1}^c \mathfrak{R}_n(\mathcal{H}_y) + M \sqrt{\frac{\log \frac{2}{\delta}}{2n}}.
\end{aligned} \tag{34}$$

which concludes the proof.

Table 8: Predictive performance of each comparing approach (mean \pm std) in terms of *Ranking loss* \downarrow . The best performance (the smaller the better) is shown in bold face.

Datasets	SMILE	AN	AN-LS	WAN	ROLE	GLOCAL	MLML	D2ML
CAL500	0.239\pm0.010	0.266 \pm 0.045	0.391 \pm 0.048	0.244 \pm 0.005	0.384 \pm 0.010	0.366 \pm 0.009	0.478 \pm 0.001	0.506 \pm 0.013
image	0.170 \pm 0.055	0.330 \pm 0.092	0.325 \pm 0.084	0.240 \pm 0.045	0.234 \pm 0.034	0.179 \pm 0.004	0.163\pm0.003	0.459 \pm 0.014
scene	0.086 \pm 0.045	0.170 \pm 0.132	0.171 \pm 0.119	0.108 \pm 0.014	0.163 \pm 0.045	0.108 \pm 0.006	0.056\pm0.007	0.383 \pm 0.035
yeast	0.161\pm0.003	0.165 \pm 0.002	0.168 \pm 0.002	0.163 \pm 0.001	0.168 \pm 0.001	0.332 \pm 0.007	0.361 \pm 0.000	0.488 \pm 0.007
corel5k	0.134 \pm 0.003	0.113 \pm 0.001	0.189 \pm 0.011	0.111\pm0.001	0.266 \pm 0.013	0.139 \pm 0.002	0.355 \pm 0.003	0.484 \pm 0.001
rev1-s1	0.042\pm0.000	0.046 \pm 0.001	0.060 \pm 0.001	0.042 \pm 0.000	0.071 \pm 0.004	0.168 \pm 0.003	0.179 \pm 0.007	0.437 \pm 0.002
corel16k-s1	0.133\pm0.001	0.138 \pm 0.002	0.181 \pm 0.002	0.134 \pm 0.001	0.241 \pm 0.006	0.690 \pm 0.001	0.306 \pm 0.005	0.454 \pm 0.002
delicious	0.126 \pm 0.000	0.133 \pm 0.002	0.276 \pm 0.015	0.125\pm0.001	0.306 \pm 0.007	0.445 \pm 0.011	0.325 \pm 0.004	0.456 \pm 0.004
iaprtc12	0.115\pm0.002	0.128 \pm 0.003	0.230 \pm 0.011	0.140 \pm 0.005	0.167 \pm 0.002	0.442 \pm 0.003	0.266 \pm 0.011	0.502 \pm 0.015
espgame	0.158\pm0.001	0.163 \pm 0.006	0.268 \pm 0.004	0.158 \pm 0.001	0.241 \pm 0.006	0.464 \pm 0.001	0.319 \pm 0.023	0.500 \pm 0.003
mirflickr	0.117\pm0.002	0.118 \pm 0.001	0.148 \pm 0.003	0.123 \pm 0.002	0.155 \pm 0.006	0.189 \pm 0.019	0.944 \pm 0.003	0.496 \pm 0.007
tmc2007	0.049 \pm 0.001	0.047 \pm 0.001	0.060 \pm 0.002	0.045\pm0.001	0.061 \pm 0.002	0.144 \pm 0.003	0.143 \pm 0.001	0.453 \pm 0.001

Table 9: Predictive performance of each comparing approach (mean \pm std) in terms of *Coverage* \downarrow . The best performance (the smaller the better) is shown in bold face.

Datasets	SMILE	AN	AN-LS	WAN	ROLE	GLOCAL	MLML	D2ML
CAL500	0.865 \pm 0.008	0.881 \pm 0.014	0.937 \pm 0.017	0.878 \pm 0.015	0.953 \pm 0.012	0.875 \pm 0.013	0.668\pm0.001	0.694 \pm 0.003
image	0.171\pm0.045	0.298 \pm 0.075	0.294 \pm 0.069	0.225 \pm 0.037	0.221 \pm 0.028	0.177 \pm 0.018	0.783 \pm 0.005	0.966 \pm 0.014
scene	0.084\pm0.037	0.155 \pm 0.112	0.156 \pm 0.101	0.102 \pm 0.012	0.146 \pm 0.036	0.103 \pm 0.002	0.414 \pm 0.002	0.931 \pm 0.004
yeast	0.455\pm0.007	0.456 \pm 0.008	0.469 \pm 0.010	0.460 \pm 0.004	0.476 \pm 0.004	0.689 \pm 0.001	0.942 \pm 0.003	0.951 \pm 0.002
corel5k	0.312 \pm 0.007	0.273\pm0.002	0.447 \pm 0.022	0.273 \pm 0.001	0.557 \pm 0.025	0.328 \pm 0.005	0.396 \pm 0.008	0.465 \pm 0.016
rev1-s1	0.107\pm0.001	0.117 \pm 0.003	0.153 \pm 0.004	0.107 \pm 0.000	0.177 \pm 0.007	0.315 \pm 0.004	0.439 \pm 0.002	0.731 \pm 0.003
corel16k-s1	0.269\pm0.003	0.280 \pm 0.006	0.364 \pm 0.005	0.271 \pm 0.001	0.465 \pm 0.010	0.847 \pm 0.007	0.740 \pm 0.004	0.848 \pm 0.006
delicious	0.630 \pm 0.002	0.647 \pm 0.012	0.894 \pm 0.013	0.626\pm0.003	0.910 \pm 0.004	0.861 \pm 0.009	0.749 \pm 0.019	0.829 \pm 0.002
iaprtc12	0.336\pm0.003	0.361 \pm 0.007	0.593 \pm 0.019	0.377 \pm 0.010	0.446 \pm 0.005	0.695 \pm 0.011	0.793 \pm 0.007	0.934 \pm 0.008
espgame	0.382\pm0.004	0.395 \pm 0.017	0.603 \pm 0.009	0.384 \pm 0.002	0.556 \pm 0.012	0.721 \pm 0.018	0.850 \pm 0.004	0.935 \pm 0.006
mirflickr	0.327\pm0.003	0.328 \pm 0.003	0.397 \pm 0.005	0.332 \pm 0.002	0.396 \pm 0.013	0.436 \pm 0.016	0.944 \pm 0.012	0.990 \pm 0.003
tmc2007	0.130 \pm 0.002	0.124 \pm 0.002	0.149 \pm 0.004	0.120\pm0.001	0.150 \pm 0.004	0.264 \pm 0.004	0.834 \pm 0.003	0.985 \pm 0.000

F Details of Experiments

Some basic statistics about these datasets are given in Table 6, including the number of examples ($|S|$), the number of features ($\dim(S)$), and the number of class labels ($L(S)$). Tables 7 to 9 show the results of all approaches on *One-error*, *Hamming loss*, and *Coverage*, respectively. Tables 10 shows the results of SMILE and its variant SMILE-SI (mean \pm std) in terms of *Hamming Loss* and *Coverage*.

Table 10: Predictive performance of SMILE and its variant (mean \pm std) in terms of *Hamming Loss* and *Coverage*.

Datasets	<i>Hamming loss</i> \downarrow		<i>Coverage</i> \downarrow	
	SMILE	SMILE-SI	SMILE	SMILE-SI
CAL500	0.148\pm0.000	0.148 \pm 0.000	0.865\pm0.008	0.897 \pm 0.002
image	0.205\pm0.008	0.229 \pm 0.000	0.171\pm0.045	0.376 \pm 0.007
scene	0.124\pm0.035	0.169 \pm 0.008	0.084\pm0.037	0.152 \pm 0.030
yeast	0.205\pm0.003	0.306 \pm 0.000	0.455\pm0.007	0.457 \pm 0.003
corel5k	0.010\pm0.000	0.010 \pm 0.000	0.312 \pm 0.007	0.282\pm0.001
rcv1-s1	0.027\pm0.000	0.029 \pm 0.000	0.107\pm0.001	0.138 \pm 0.001
corel16k-s1	0.019\pm0.004	0.019 \pm 0.000	0.269\pm0.003	0.283 \pm 0.000
delicious	0.019\pm0.001	0.019 \pm 0.000	0.630\pm0.002	0.663 \pm 0.005
iaprtc12	0.019\pm0.011	0.019 \pm 0.000	0.336\pm0.003	0.403 \pm 0.000
espgame	0.017\pm0.003	0.017 \pm 0.000	0.382\pm0.004	0.412 \pm 0.005
mirflickr	0.118\pm0.001	0.128 \pm 0.000	0.327\pm0.003	0.335 \pm 0.002
tmc2007	0.063\pm0.000	0.098 \pm 0.000	0.130 \pm 0.002	0.127\pm0.000